Research Paper

Journal of Vascular Research

J Vasc Res 2012;49:329–341
DOI: 10.1159/000337463

Received: September 6, 2011
Accepted after revision: February 5, 2012
Published online: May 23, 2012

The Most Negatively Charged Low-Density Lipoprotein L5 Induces Stress Pathways in Vascular Endothelial Cells

Ching-Yi Chen[a] Hsiu-Ching Hsu[b] An-Sheng Lee[d, e] Daming Tang[f] Lu-Ping Chow[c] Chao-Yuh Yang[d–f] Han Chen[g] Yuan-Teh Lee[b, d] Chu-Huang Chen[d–g]

[a]Department of Animal Science and Technology, [b]Department of Internal Medicine, College of Medicine, and [c]Graduate Institute of Biochemistry and Molecular Biology, College of Medicine, National Taiwan University, Taipei, [d]China Medical University, and [e]L5 Research Center, China Medical University Hospital, Taichung, Taiwan, ROC; [f]Department of Medicine, Baylor College of Medicine, and [g]Vascular and Medicinal Research, Texas Heart Institute at St. Luke's Episcopal Hospital, Houston, Tex., USA

Key Words
Atherogenesis · Endoplasmic reticulum stress · L5 · Mitochondrial stress · RNA destabilization

Abstract
Background/Aims: L5, the most negatively charged species of low-density lipoprotein (LDL), has been implicated in atherogenesis by inducing apoptosis of endothelial cells (ECs) and inhibiting the differentiation of endothelial progenitor cells. In this study, we compared the effects of LDL charge on cellular stress pathways leading to atherogenesis. ***Methods:*** We isolated L5 and L1 (the least negatively charged LDL) from the plasma of patients with familial hypercholesterolemia and used JC-1 staining to examine the effects of L5 and L1 on the mitochondrial membrane potential (DCm) in human umbilical vein ECs (HUVECs). Additionally, we characterized the gene expression profiles of 7 proteins involved in various types of cellular stress. ***Results:*** The DCm was severely compromised in HUVECs treated with L5. Furthermore, compared with L1, L5 induced a decrease in mRNA and protein expression of the endoplasmic reticulum (ER) chaperone proteins ORP150, Grp94, and Grp58, mitochondrial proteins Prdx3 and ATP synthase, and an increase in the expression of the pro-inflammatory protein hnRNP C1/C2. ***Conclusions:*** Our work suggests that L5, but not L1, may promote the destruction of ECs that occurs during atherogenesis by causing mitochondrial dysfunction and modulating the expression of key proteins to promote inflammation, ER dysfunction, oxidative stress, and apoptosis.

Introduction

Cellular stress plays a crucial role in the development of atherosclerosis. Oxidative stress, one of the main factors in the process of atherogenesis, is caused by reactive oxygen species that induce inflammation, promote leukocyte recruitment, and inhibit endothelial cell (EC) proliferation [1–4]. Furthermore, oxidative stress induced in the mitochondria causes the accumulation of mitochondrial DNA damage and the progressive dysfunction of the respiratory chain, which results in apoptosis and fa-

KARGER
Fax +41 61 306 12 34
E-Mail karger@karger.ch
www.karger.com

1018–1172/12/0494–00329$38.00/0

Accessible online at:
www.karger.com/jvr

Dr. Chu-Huang Chen
Vascular and Medicinal Research, Texas Heart Institute
6770 Bertner Avenue, MC 2-255
Houston, TX 77030-2604 (USA)
Tel. +1 832 355 9026, E-Mail cchen@heart.thi.tmc.edu

vors plaque rupture [5]. By providing antioxidant activity and promoting ATP synthesis, respectively, thioredoxins and ATP synthase protect cells from oxidative damage and increase ATP levels to maintain normal mitochondrial functions [6–8]. The family of heterogeneous nuclear ribonucleoproteins (hnRNPs) is also involved in the response to oxidative stress: by specifically binding RNA motifs, hnRNPs stabilize mRNA transcripts such as endothelial nitric oxide synthase and vascular endothelial growth factor (VEGF) and regulate protein expression under oxidative stress [9, 10].

Endoplasmic reticulum (ER) stress also contributes to atherogenesis. In advanced atherosclerosis, the accumulation of free cholesterol induces ER stress that causes macrophage apoptosis, stimulates inflammation in vulnerable plaque, and promotes plaque destabilization [11, 12]. In addition, the accumulation of misfolded/damaged proteins that aggregate in the lumen of the ER causes ER stress and dysfunction. Glucose-related proteins (GRPs), located in the lumen of the ER, are responsible for properly folding proteins and degrading misfolded/ubiquitinated proteins. Under normal conditions, GRPs are induced when ER stability is threatened to prevent ER stress-induced cell death [13–15].

Human plasma LDL can be chromatographically divided by charge into 5 subfractions, L1–L5. L5 is the most negatively charged LDL subfraction found in the circulation of individuals with risk factors for coronary artery disease, including hypercholesterolemia [15–19]. L5 has been shown to have biologic effects similar to those of oxidized LDL (ox-LDL), which is oxidized in vitro. L5 and ox-LDL are more electronegative than unoxidized LDL, and electronegative LDL contains higher proportions of conjugated dienes and thiobarbituric acid [20]. Copper-oxidized LDL distinctively contains products of modified apolipoprotein (apo) B100, whereas L5 contains primarily apoB100, as well as apoCIII, apoAI, and apoE [15, 16].

We previously showed that L5 is potentially atherogenic, evident by its ability to induce inflammation, EC dysfunction, leukocyte recruitment, monocyte differentiation, smooth muscle cell proliferation, and foam cell formation [15–17, 21]. We also found that atheroma-derived LDL induced oxidative stress and ER stress in human umbilical vein ECs (HUVECs) when compared to native LDL [22].

The results of the present study further indicate a role for L5 in inducing cellular stress that can lead to atherogenesis. We show evidence that L5 promotes inflammation, mitochondrial dysfunction, and reduced cell viability, whereas L1 does not. Furthermore, we compared the mRNA and protein expression profiles of 7 stress-related proteins in HUVECs treated with either L5 or L1. Given that these proteins are known to function in RNA metabolism, repair of the ER, and the mitochondria, we discuss how L5 may orchestrate downstream signaling that leads to atherogenesis.

Subjects and Methods

Subjects

Our study conforms to the principles outlined in the Declaration of Helsinki. We isolated LDL from the plasma of patients with homozygotic familial hypercholesterolemia (2 women, 33 and 41 years old, and 1 boy, 6 years old) [16, 21]. All donors gave informed consent.

Isolation of LDL Subfractions

We separated LDL from the plasma of patients into subfractions (L1–L5) by using anion exchange chromatography [15, 16, 22].

Cell Culture

HUVECs were grown in supplemented M199 medium (Biochrom AG) in a humidified atmosphere containing 5% CO_2. Cells were propagated by trypsin digestion at the confluent stage and used for experiments between passages 3 and 5 [22].

Cell Treatment

HUVECs grown to 90% confluence were maintained in medium containing 5% fetal calf serum and were treated with phosphate-buffered saline (PBS) or 50 μg/ml of L1 or L5 for 24 h as previously described [22].

Detection of Monocyte Chemotactic Protein-1

Monocyte chemotactic protein-1 (MCP-1), an indicator of inflammation, was detected either by Western blot (described below) or by using an enzyme-linked immunosorbent assay (ELISA) kit (BioSource). MCP-1 secreted into the medium was measured and estimated spectrophotometrically at 450 nm.

Western Blotting

Preparation of whole-cell lysates and Western blotting was performed as described previously [22]. Antibodies specific for GAPDH, Grp58, Grp78, Grp94, ORP150, ATP synthase, hnRNP C1/C2, peroxiredoxin 3 (Prdx3), inositol-requiring enzyme 1 (IRE-1), and phosphorylated protein kinase RNA-like ER kinase (p-PERK; Santa Cruz Biotechnology) were used to detect the corresponding proteins. Signals were visualized and quantified by using Quantity One software (Amersham Biosciences).

Cell Viability

As previously described [22], cell viability was measured by using the MTT [3-(4,5-dimethyl-2-yl)-2,5-diphenyltetrazolium bromide] method. HUVECs were grown in 24-well plates at a density of 5×10^4 cells/well. Cells grown to 90% confluence were treated with PBS, L1, or L5 (50 μg/ml each) for 24 h, washed, and incubated with MTT (0.5 mg/ml) for 8 h. DMSO (1 ml) was then

Table 1. Proteomic identification of proteins in HUVECs treated with L1 or L5

No.	Protein ID[a]	NCBI No.	Theoretical MW/PI, kDa	Observed MW/PI, kDa	Matching mass n	Matching mass n	m/z	Size	Amino acid sequences	Sequence coverage, %	Mowse score[b]
1	ORP150	gi5453832	111.2/5.16	110.0/4.95	7	4	1515.7226	120–131	FFEHELTFDPQR	5.7	52
							1047.5581	283–291	LAGLFNEQR		
							1521.8311	439–451	DAVVYFILYEFTR		
							2726.2633	487–509	YSHDFNFHINYGDLGFLGFEDLR		
2	Grp94	gi4507677	92.4/4.76	94.8/4.80	15	2	1081.5511	55–63	FAFQAEVNR	3.5	
							2262.0488	491–509	FQSSHHFTDITSLDQYVER		
3	Grp78	gi6900104	72.3/5.07	73.7/5.40	7	2	1555.7935	47–60	GRYEILANDQGN	4.6	
							1833.9089	82–97	NQLTSNFENTYFDAKR		
4	Grp58	gi1085373	56.6/5.88	62.0/5.90	9	5	2703.4000	305–329	KTFSHELSDFGLESTAGETTPVVAIR	12.5	197
							2575.3000	306–329	TFSHELSDFGLESTAGEIPVVAER		
							1515.8000	352–363	FLQDYFDGNLKR		
							1780.8185	396–410	DVLIEFYAFWCGHCK		
							1370.7000	472–482	ELSDFISYLQR		
							1173.7000	336–344	FVMQEEFSR		
5	hnRNP C1/C2	gil4758544	31.9/5.10	40.6/5.00	7	1	1329.6586	51–61	GFAFVQYYNER	3.8	38
6	ATP synthase	gi5453559	18.5/5.21	22.4/5.15	6	2	1872.9854	10–25	TIDWYAFAETTPQNQK	18.0	39
							1684.8482	149–161	KYPYWPHQPIENL		
7	Prdx3	gi32483377	25.8/7.04	29.6/6.30	7	2	1206.6589	179–189	HLSVNDLFVGR	8.0	37
							1055.5156	231–238	EYFQKVNQ		

[a] Trypsin-digested proteins were identified by MALDI-MS/ML.

b Mowse scores calculated by summation of the ion scores using MASCOT for the individual identified peptide sequence. An individual ion score >40 indicates identity or extensive homology ($p < 0.05$). m/z = Mass-to-charge ratio.

added to solubilize the formazan salt, which was measured spectrophotometrically at 562 nm. The data, calculated relative to L1, represent the mean from 5 independent experiments. $p < 0.05$ was considered significant.

JC-1 Staining and Flow Cytometry

Changes in the mitochondrial membrane potential (DCm) after different treatments were studied by staining with the cationic dye JC-1 (5,5′,6,6′-tetrachloro-1,1′,3,3′-tetraethylbenzimidazolcarbocyanine iodide). JC-1 accumulates in the mitochondria of healthy cells and fluoresces red (560 nm). When the DCm collapses, JC-1 uptake is limited to the cytoplasm where it fluoresces green (530 nm). Hence, a collapse in the DCm is indicated by a reduction in the red/green fluorescence-intensity ratio. HUVECs were pretreated with PBS or 50 μg/ml of L1 or L5 for 1 h in a cell culture incubator and then incubated with 10 mg/ml JC-1 (Sigma-Aldrich Biotechnology) for 20 min at room temperature. Cells were washed twice with PBS and observed by fluorescence microscopy (Delta Vision, Applied Precision).

In a parallel experiment, cells treated in the same manner as above were digested with trypsin, washed twice with PBS, and then analyzed on an LSR flow cytometer (Becton Dickinson) to detect green fluorescence at excitation/emission wavelengths of 485/530 nm and red fluorescence at excitation/emission wavelengths of 485/590 nm.

Two-Dimensional Electrophoresis and Image Analysis

Two-dimensional (2-D) electrophoresis was performed as described previously [22]. Although over 50 proteins were originally identified to have altered expression in response to L5 [22], only 7 proteins related to cellular stress are examined in this study (table 1): ER proteins Grp94, Grp78, Grp58, and ORP150; RNA-related protein hnRNP C1/C2; and mitochondrial proteins ATP synthase and Prdx3. Protein spots were detected automatically and confirmed manually; then, the volume of each spot was normalized as a fraction of the volume of all the spots on the gel and expressed relative to the same value for the L1 group. Each intergroup comparison of samples was carried out on 4 replicate gels.

In-Gel Digestion and Mass Spectrometry

Protein spots were destained, dehydrated, and digested with trypsin as previously described [22]. Peptides were eluted in 0.8 ml of matrix solution (α-cyano-4-hydroxy cinnamic acid; 8 mg/ml in 70% v/v acetonitril/1% formic acid) directly onto a target plate and subjected to analysis by mass spectrometry. A QStar hybrid quadrupole time-of-flight mass spectrometer (QTOF; Applied Biosystems) equipped with a matrix-assisted laser desorption ionization (MALDI) source and a nitrogen laser (337 nm) was used to acquire MALDI-MS and -MS/MS spectra. The MS/MS spectra were used to automatically search the NCBInr protein da-

tabase by using MASCOT software (http://www.matrixscience.com/). Parameters used for identification were described previously [22].

Reverse Transcription Polymerase Chain Reaction

RNA was isolated from ECs by using RNAzol (TEL-TEST). One microgram of total RNA was used for reverse transcription with PowerScript reverse transcriptase (Clontech), oligo-dT primers, and random primers. One-twentieth of the cDNA was then used as template for PCR. Amplification of cDNA was performed in 50 μl of PCR Master Mix (Becton Dickinson) containing 10 μM forward primers and reverse primers and approximately 50 ng of cDNA. PCR cycling parameters were as follows: 1 cycle at 94°C for 1.5 min, and 30 cycles at 94°C for 30 s, 64°C for 30 s, and 72°C for 1 min. The primer sequences for the genes examined were

(1) Grp58: forward primer 5′-CGAATGTTGAGTCTCTGGTGAA-3′ and reverse primer 5′-CAAAGTAATCCTGCAGGAACCT-3′, which amplified a 513-bp cDNA fragment;
(2) Grp78: forward primer 5′-CTCGAATTCCAAAGATTCAGCAACT-3′ and reverse primer 5′-CTCCACAGTTTCAATACCAAGTG-3′, 299 bp;
(3) Grp94: forward primer 5′-CAGGAAGATGGCCAGTCAACT-3′ and reverse primer 5′-GATGGTCTCTGCCATATTGGTT-3′, 497 bp;
(4) ORP150: forward primer 5′-ACACTCCGAGACCTGGAGAA-3′ and reverse primer 5′-CAACACAGGCTTCTCTGTGG-3′, 480 bp [23];
(5) Prdx3: forward primer 5′-CGCACTCTTAGACTTAACT-3′ and reverse primer 5′-CATAATTGGTTCCTTGCCTTCTA-3′, 406 bp;
(6) ATP synthase: forward primer 5′-GGTCGGTGAAGGATCCCAAAA-3′ and reverse primer 5′-CAAGTCCTCAATGGTCATCTGA-3′, 428 bp;
(7) hnRNP C1/C2: forward primer 5′-GCAGGTGTGAAACGATCTGCA-3′ and reverse primer 5′-CCTTGATCAACTCCAGCTGGT-3′, 532 bp, and
(8) GAPDH: forward primer 5′-ACAACTCTCTCAAGATTGTCAGCAA-3′ and reverse primer 5′-ACTTTGTGAAGCTCATTTCCTGG-3′, 518 bp.

Statistical Analysis

The differences observed between LDL subfractions L1 and L5 were compared by analysis of variance using SAS software (version 9.0; SAS Institute), followed by a post hoc Dunnett test. All data are expressed as mean ± SEM, and the differences were considered significant at $p < 0.05$.

Results

Effect of L1 and L5 on MCP-1 Expression, Cell Viability, and Mitochondrial Dysfunction

The secretion of MCP-1 was used as an indicator of inflammation. The dose effect of L5 and L1 on the inflammatory response of HUVECs is shown in figure 1a (50 μg/ml, $p < 0.05$; 100 μg/ml, $p < 0.01$; $n = 5$). Because 50 μg/ml of L5 sufficiently induced inflammation, this concentration was used in subsequent experiments.

Cells treated with L5 showed a 3-fold increase in MCP-1 expression, whereas treatment with L1 (50 μg/ml) did not affect MCP-1 expression (fig. 1b). In parallel, ELISA analysis revealed that treating cells with L5 markedly increased the concentration of MCP-1 detected in cell lysates (>2,000 pg/10^5 cells; $p < 0.05$), whereas L1 exhibited no effect (L1, 125 ± 79 pg/10^5 cells vs. PBS, 157 ± 55 pg/10^5 cells; fig. 1c).

Cell viability was determined by the MTT assay. The viability of cells treated with L5 was calculated as the relative ratio to the number of cells surviving L1 treatment. In cells treated with L5, viability was 25% less than in cells treated with L1, suggesting that L5 decreased cell survivability compared to L1.

Mitochondrial function was assessed by the color and pattern of JC-1 immunofluorescence staining (fig. 1d). Red (indicative of normal mitochondrial function) and green cytoplasmic fluorescence staining were observed in HUVECs treated with either PBS or L1. However, cells treated with L5 showed a marked reduction in red fluorescence and a reciprocal increase in green fluorescence, suggesting loss of DCm. A similar reduction in red fluorescence was observed by flow cytometry in the presence of L5, but not L1 (fig. 1e).

Protein Expression Profiles of HUVECs Treated with L1 or L5

The protein expression profiles of HUVECs treated with PBS, L1, or L5 were studied by 2-D electrophoresis and mass spectrometry (fig. 2a). The relative amounts of proteins expressed were quantified with the use of ImageMaster software (fig. 2b) and calculated as the relative ratio to L1 (L1 treatment = 1). Compared to treatment with L1, treatment of HUVECs with L5 significantly upregulated hnRNP C1/C2 expression (1.49 ± 0.12 vs. 1.00 ± 0.14; $p < 0.05$) and downregulated the expression of Grp58, Grp78, Grp94, ATP synthase, and Prdx3 (0.77 ± 0.06 vs. 1.00 ± 0.06, 0.81 ± 0.08 vs. 1.00 ± 0.08, 0.70 ± 0.11 vs. 1.00 ± 0.11, 0.75 ± 0.10 vs. 1.00 ± 0.10, 0.65 ± 0.08 vs. 1.00 ± 0.09, respectively; $p < 0.05$, $n = 4$); there was also a nonsignificant reduction in ORP150 expression (0.89 ± 0.39 vs. 1.00 ± 0.39). These results are similar to those previously observed when L5 and LDL derived from normal volunteers were compared [22]. Figure 3a shows an example of MALDI-QTOF performed for spot 4, which identifies a 'fingerprint' spectrum of peptides. Figure 3b–f are MS/MS spectra of spot 4, which was identified as Grp58.

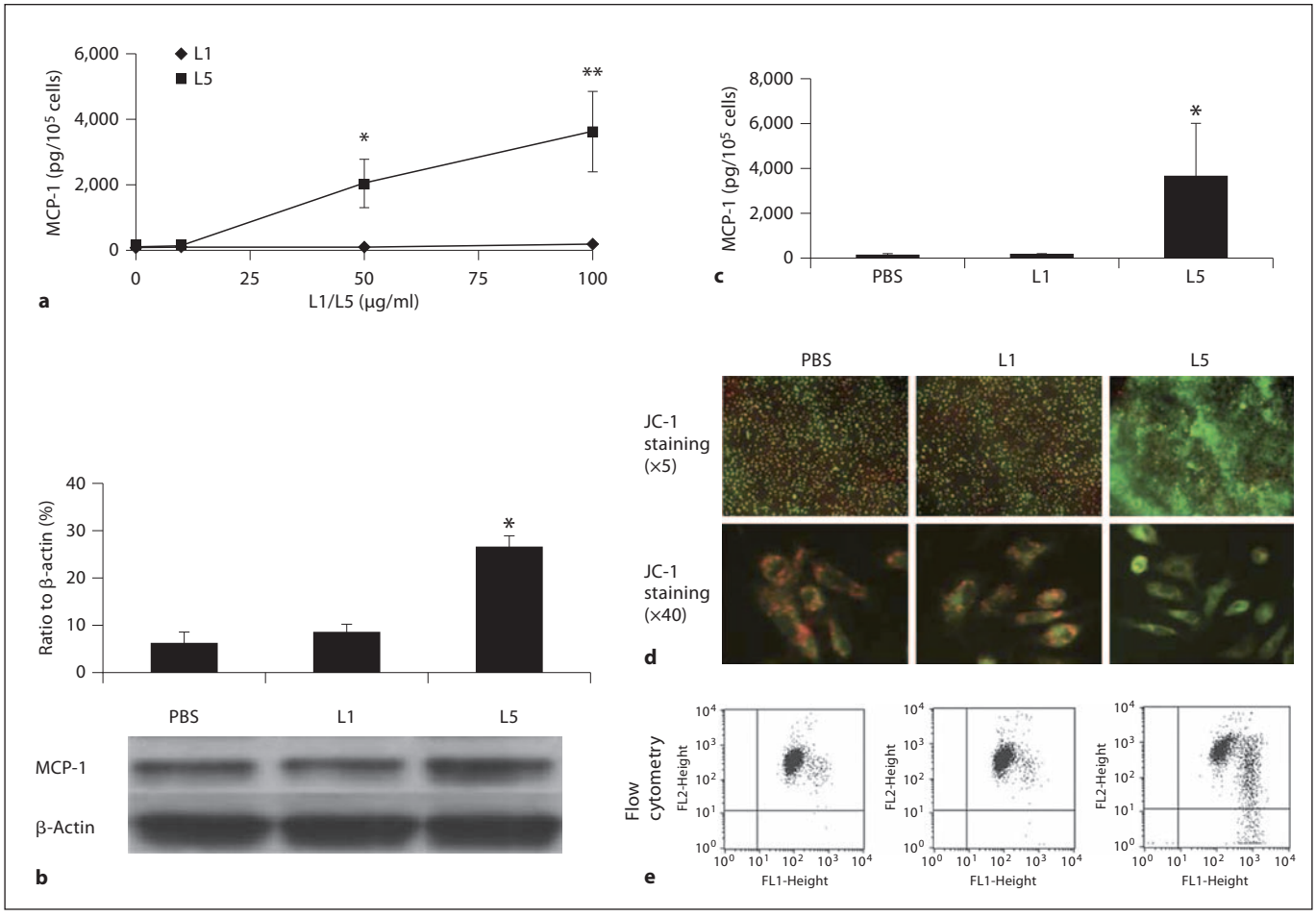

Fig. 1. a Concentration-dependent effect of L5 on MCP-1 levels. **b**, **c** Induction of MCP-1 expression examined by Western blotting of cell lysates (**b**) and ELISA of the supernatants of HUVECs (**c**). **d**, **e** Disruption of mitochondrial membrane integrity by L5 examined by immunofluorescence microscopy (**d**) and flow cytometry (**e**). * $p < 0.05$, ** $p < 0.01$; n = 5.

Effect of L1 and L5 on Gene and Protein Expression in HUVECs

We used RT-PCR to examine the expression of these 7 genes in HUVECs treated with PBS, L1, or L5 (fig. 4a). Gene expression in cells treated with L5 was calculated as the relative ratio to gene expression in cells treated with L1 (L1 treatment = 1). Treatment of HUVECs with L5 significantly decreased gene expression of Grp58, Grp94, ORP150, Prdx3, and ATP synthase relative to L1 (0.70 ± 0.15 vs. 1.00 ± 0.14, 0.11 ± 0.28 vs. 1.00 ± 0.24, 0.66 ± 0.14 vs. 1.00 ± 0.16, 0.83 ± 0.07 vs. 1.00 ± 0.08, 0.76 ± 0.13 vs. 1.00 ± 0.11, respectively; $p < 0.05$). In addition, L5 significantly increased gene expression of hnRNP C1/C2 relative to L1 (1.34 ± 0.13 vs. 1.00 ± 0.15; $p < 0.05$). The decrement in Grp78 expression observed in cells treated with L5 was not statistically significant.

Immunoblotting of protein expression corroborated the findings from the 2-D analysis, showing a consistent pattern of protein expression (fig. 4b) for cells treated with L1 or L5. The results of immunoblotting revealed that L5 significantly reduced the expression of Grp94, Grp58, ORP150, ATP synthase, and Prdx3 relative to L1 (0.62 ± 0.11 vs. 1.00 ± 0.13, 0.70 ± 0.08 vs. 1.00 ± 0.08, 0.67 ± 0.06 vs. 1.00 ± 0.08, 0.80 ± 0.07 vs. 1.00 ± 0.09, 0.72 ± 0.13 vs. 1.02 ± 0.11, respectively; $p < 0.05$ or $p < 0.01$), whereas L5 enhanced the expression of hnRNP C1/C2 relative to L1 (1.67 ± 0.26 vs. 1.07 ± 0.23; $p < 0.01$). A significant change was not observed for the protein expression of Grp78.

To confirm the ER stress response following L5 treatment in HUVECs, we examined the expression of markers of maladaptive unfolded protein response, p-PERK

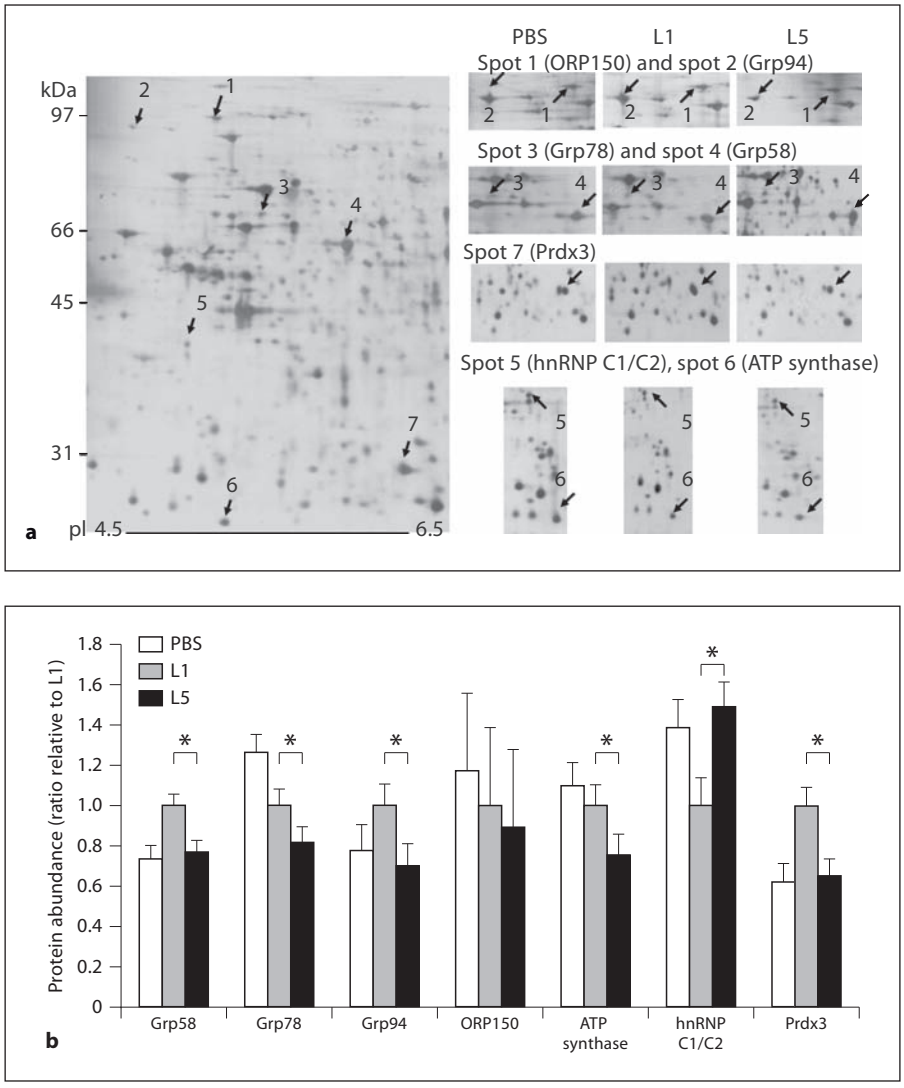

Fig. 2. Proteomic analysis of proteins expressed in HUVECs treated with PBS, L1, or L5. **a** 2-D electrophoresis of proteins in L5-treated cells (left); excerpts showing proteins of interest in cells treated with PBS, L1, or L5 (right). Numbers refer to identified proteins listed in table 1. Results are representative of 4 independent experiments. **b** Quantitative analysis of the identified proteins in cells treated with PBS, L1, or L5. * $p < 0.05$; n = 4.

and IRE-1, by immunoblotting. Relative to L1, L5 significantly ($p < 0.05$) enhanced the protein expression of the ER stress sensors p-PERK and IRE-1 in HUVECs (fig. 5).

Discussion

Previously, we found that L5 purified from the plasma of hypercholesterolemic patients induced endothelial inflammation and dysfunction, leukocyte recruitment, monocyte differentiation, smooth muscle cell proliferation, and foam cell formation – all processes that contribute to atherogenesis [15, 16, 21]. We also reported that atheroma-derived LDL induced cellular stress in HUVECs [22].

In the present study, we showed that L5, but not L1, induced severe inflammation and mitochondrial dysfunction in HUVECs and decreased cell viability, possibly initializing the process of atherogenesis. The exposure of ECs to L5 induces oxidative and ER stress similar to that of atheroma-derived LDL, possibly through a mechanism involving RNA destabilization and dysfunction of the ER and the mitochondria in HUVECs.

Mitochondrial Dysfunction Induced by L5

Mitochondrial dysfunction induced by L5 is indicated by JC-1 immunofluorescence. The collapse of the DCm seen in L5-treated cells is an early characteristic feature of oxidative injury and apoptosis. Additionally, protein and mRNA levels of the mitochondrial proteins

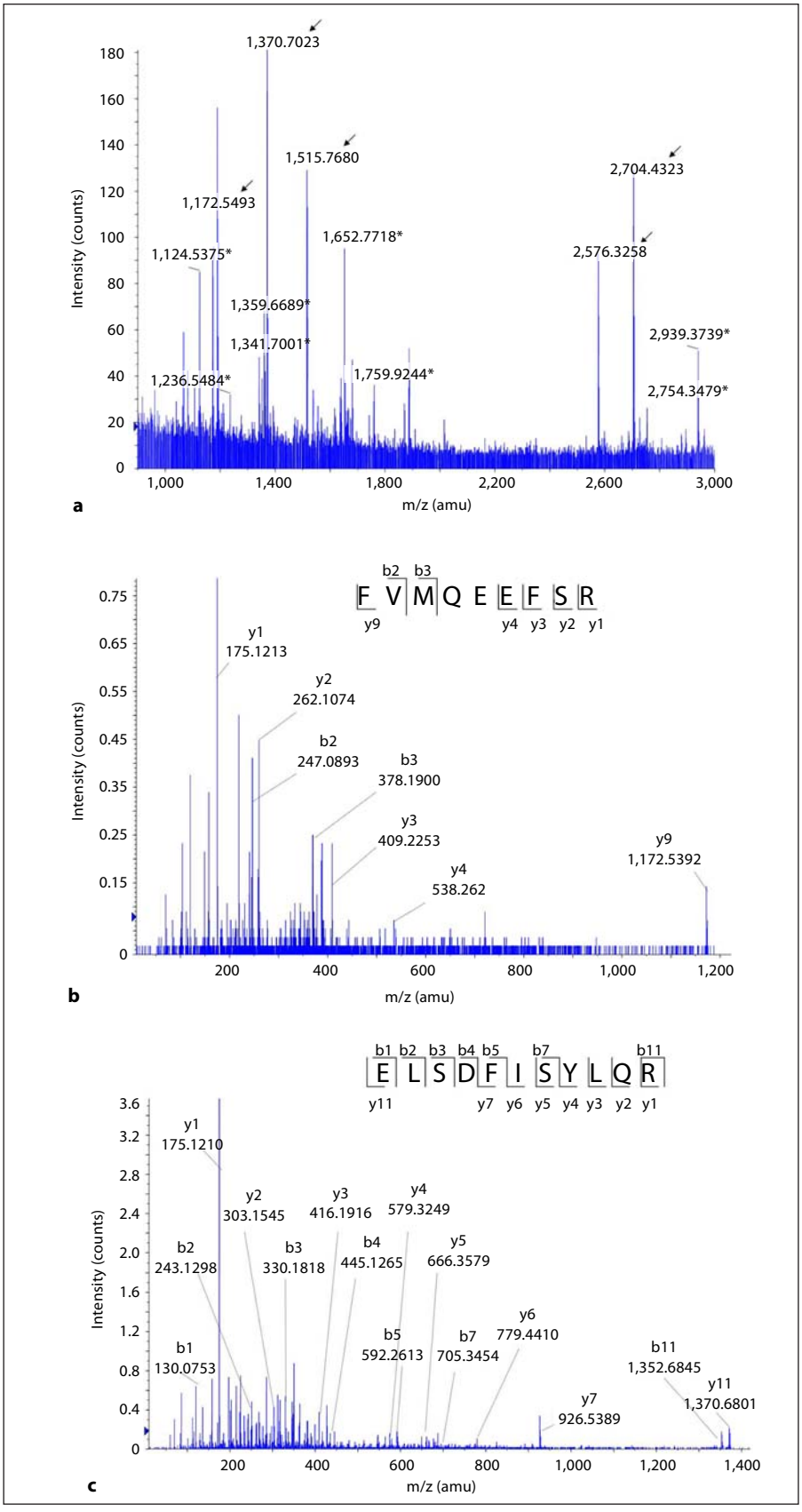

(For legend see next page.)

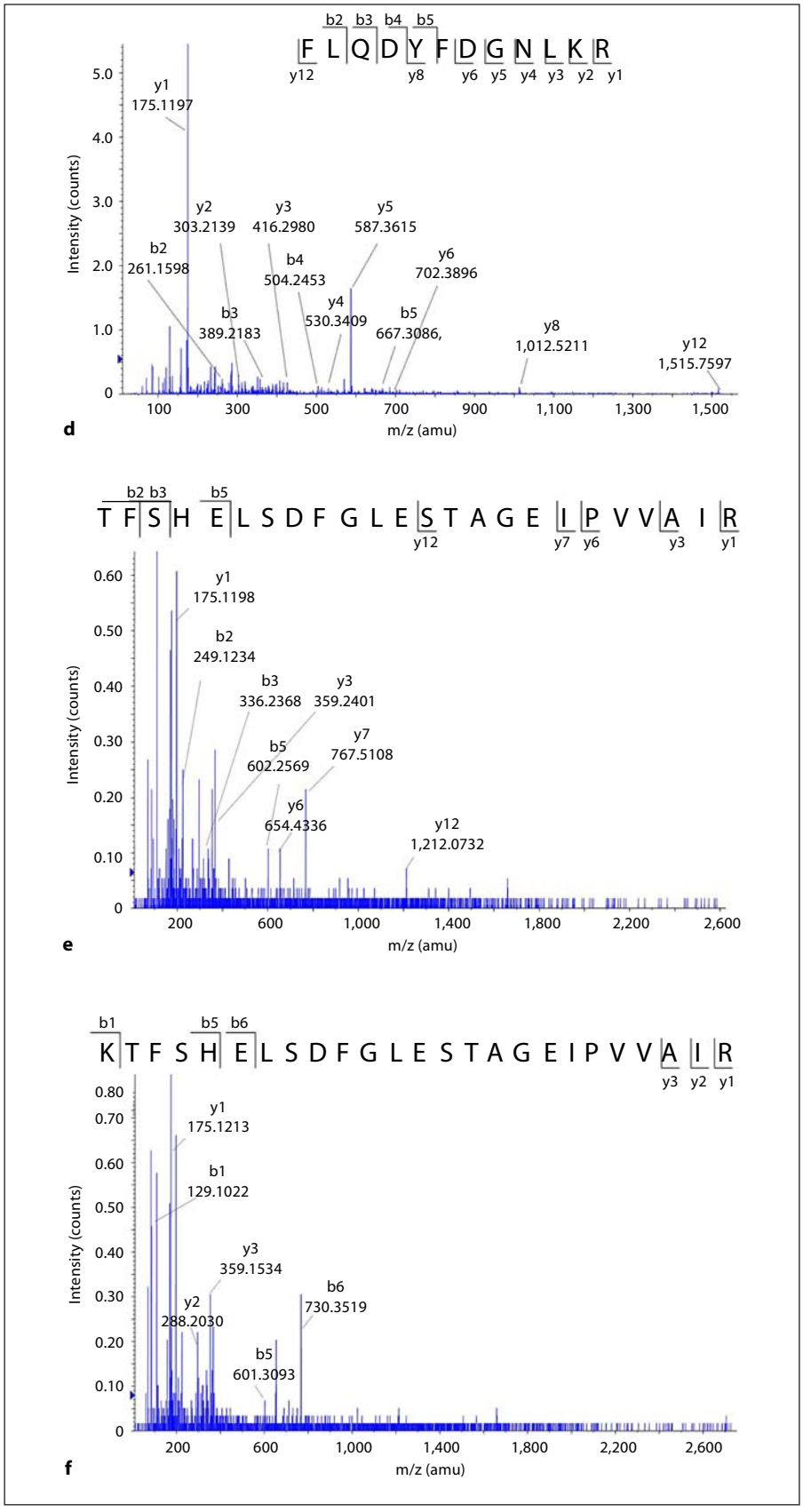

Fig. 3. Example of spot identification by MALDI-QTOF and multiple MALDI-MS/MS sequencing. **a** Identification of peptide mass fingerprint spectra of protein spot 4 by MALDI-QTOF. Arrows represent sites of MALDI-MS/MS sequencing performed to confirm protein identification. **b–f** MS/MS spectra of representative amino acid sequences. Spot 4 was identified as Grp58.

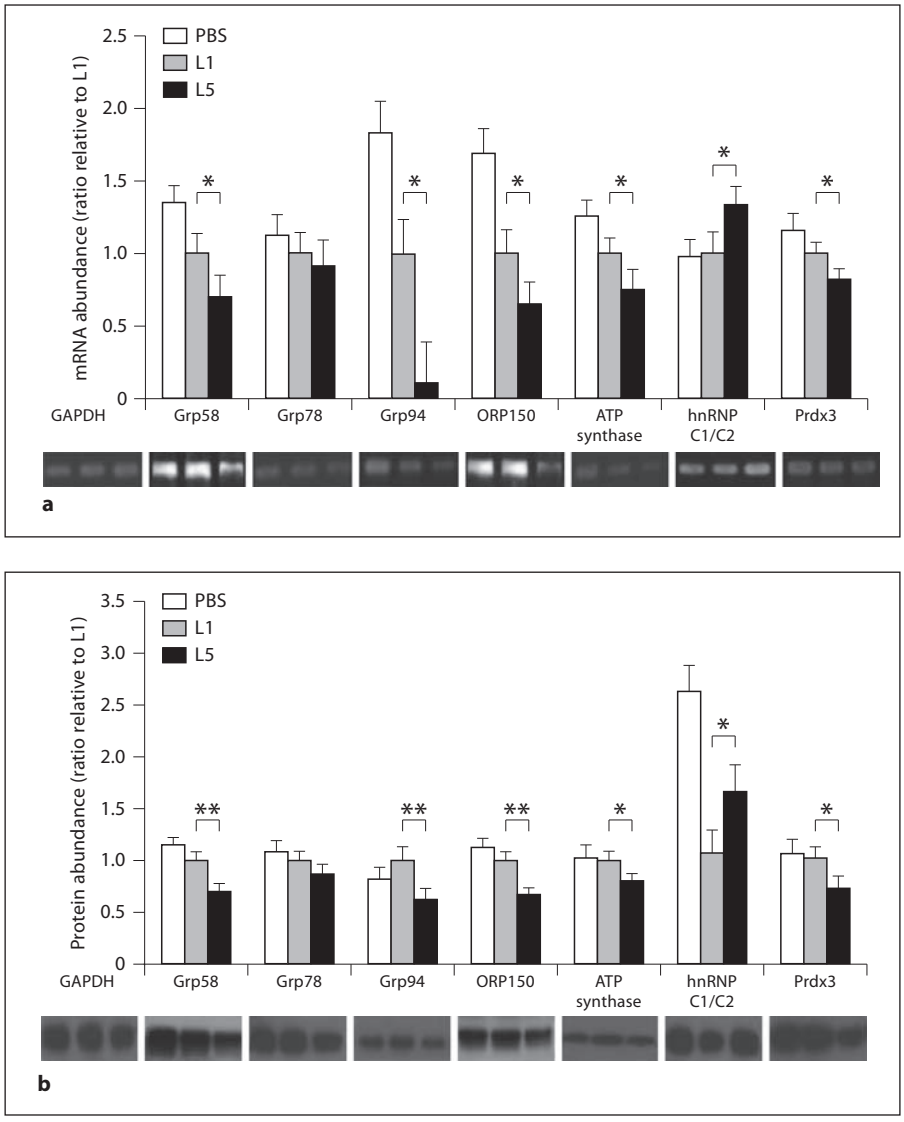

Fig. 4. RT-PCR and Western blot analysis of the indicated mRNA transcripts (**a**) and proteins (**b**) (identified in fig. 2) in HUVECs treated with PBS, L1, or L5. mRNA and protein levels are normalized to GAPDH and analyzed relative to L1. * $p < 0.05$, ** $p < 0.01$; n = 5. RT-PCR and Western blots are representative of 5 independent experiments.

ATP synthase and Prdx3 were reduced in HUVECs treated with L5. ATP synthase, abundant in the mitochondria, serves as the key enzyme for ATP synthesis. In addition, it plays an important role in protecting fibroblast growth factor 2 (FGF2) from proteolytic cleavage, stabilizing its biologic function in cell proliferation [24, 25]. ATP synthase has also been identified on the cell surface of several cell types, including human tumor cells, hepatocytes, keratinocytes, adipocytes, and ECs [26, 27]. On hepatocyte membranes, ATP synthase is a high-affinity receptor for apoAI, and it protects against atherogenesis by mediating high-density lipoprotein endocytosis and enhancing the delivery of cholesterol to the liver [27, 28]. Prdx3, a member of the antioxidant family of thioredoxin peroxidases in the mitochondria, protects cells from oxidative damage and is essential for maintaining normal mitochondrial function [6, 7]. Prdx3 also protects cells from the apoptosis-inducing effects of high levels of H_2O_2 [6, 29]. Moreover, thioredoxins have the ability to improve vascular EC function and prevent the development of atherosclerosis by reducing oxidative stress and increasing NO bioavailability [30]. Given the protective, anti-atherogenic functions of these proteins, the downregulation of ATP synthase and Prdx3 suggests a mechanism by which L5 may increase oxidative stress and mitochondrial dysfunction observed in HUVECs.

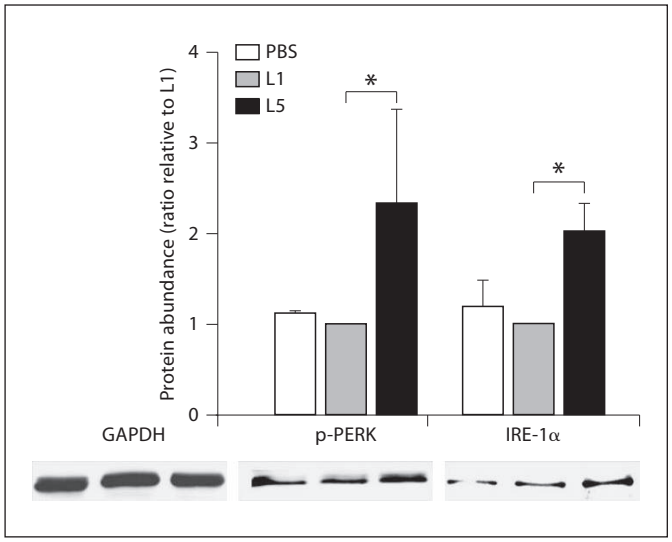

Fig. 5. Western blot analysis of the ER stress sensors p-PERK and IRE-1 in HUVECs treated with PBS, L1, or L5. p-ERK and IRE-1 protein levels are normalized to those of GAPDH and analyzed relative to L1. * $p < 0.05$; n = 3.

RNA Destabilization Induced by L5

The expression of hnRNP C1/C2 was increased in HUVECS treated with L5 when compared to those treated with L1. The hnRNP C proteins, which belong to a large family of RNA motif-binding RNPs, are among the most abundant nuclear proteins involved in mRNA biogenesis, DNA repair [31, 32], the cell cycle, apoptosis [33, 34], and the maintenance of cellular homeostasis [35]. In normal proximal internal carotid arteries, hnRNP C proteins are expressed predominantly in the endothelium, with significantly lower expression in medial smooth muscle. However, in pre-atherosclerotic intimal hyperplasia, hnRNP C proteins are upregulated in the artery wall [36].

Furthermore, oxidative stress induces hnRNP phosphorylation, which in turn modulates RNA stabilization and stimulates expression of VEGF [10, 15]. It has also been shown that angiotensin II enhances the binding of hnRNP to VEGF mRNA and increases the efficiency of VEGF mRNA translation in mice with type II diabetes [37]. In addition, VEGF has been reported to recruit macrophages to atherosclerotic plaque, resulting in the accumulation of inflammatory cells in the plaque [8]. Previously, we showed that L5 increased the expression of VEGF in ECs [21], which may occur as a result of hnRNP C1/C2 upregulation. Therefore, it is possible that inflammation of ECs may result from increased VEGF expression through hnRNP C1/C2 activation.

ER Stress Induced by L5

In addition to oxidative stress, L5, but not L1, induced ER stress by suppressing the expression of Grp58, Grp94, and ORP150. GRPs are responsible for properly folding proteins and degrading misfolded/ubiquitinated proteins and are induced during ER stress to prevent ER stress-induced cell death [13–15]. In cells exposed to L5, the reduced expression of GRPs may compromise several antiatherogenic functions of GRPs. For example, GRPs assist with the correct folding and lipidation of apoB100 during its maturation [38, 39], as well as the proteasomal degradation of apoB [40]. GRPs also modulate ER stress-induced insulin resistance [41, 42] and other related mechanisms that may directly or indirectly affect the development of atherosclerosis [43–45]. Furthermore, GRPs control the quality of newly synthesized LDL receptors by retaining mutant LDL receptors in the ER to be degraded [46] and by binding to scavenger receptor A, which regulates the receptor-mediated uptake of modified LDL into the macrophage [47].

Additionally, the ER chaperone protein ORP150 protects ECs against ER stress-induced apoptosis [48, 49]. ER stress induced by the accumulation of unfolded proteins in the ER is considered a survival pathway; however, prolonged or severe ER stress leads to programmed cell death via specific pathways originating from the ER [50]. In human mammary ECs, the expression of ORP150 protects against ER stress-induced apoptosis caused by ox-LDL, and the attenuated expression of ORP150 increases ox-LDL-induced cell death [48]. Our results show that L5 reduced the expression of ORP150, potentially promoting apoptosis through a mechanism that is similar to that of ox-LDL.

L5, but not L1, also enhanced the protein expression of the ER stress sensors p-PERK and IRE-1. The combination of the loss of DCm and the increased levels of ER stress-response sensors observed in L5-treated cells indicates that ER-initiated apoptotic signaling may play a role in the mechanism of L5-induced apoptosis.

In support of these findings, our previous studies have shown that genetically augmenting Akt, which is known to reduce ER stress, renders cells resistant to L5 [18]. In addition, we have shown that L5 induces EC apoptosis by disrupting a FGF2-PI3K-Akt autoregulation mechanism [18] and that homocysteine, an ER stress inducer, also leads to EC death by inhibiting FGF2 transcription [51]. Furthermore, our unpublished data suggest that homocysteine and L5 have synergistic effects when added simultaneously to EC cultures.

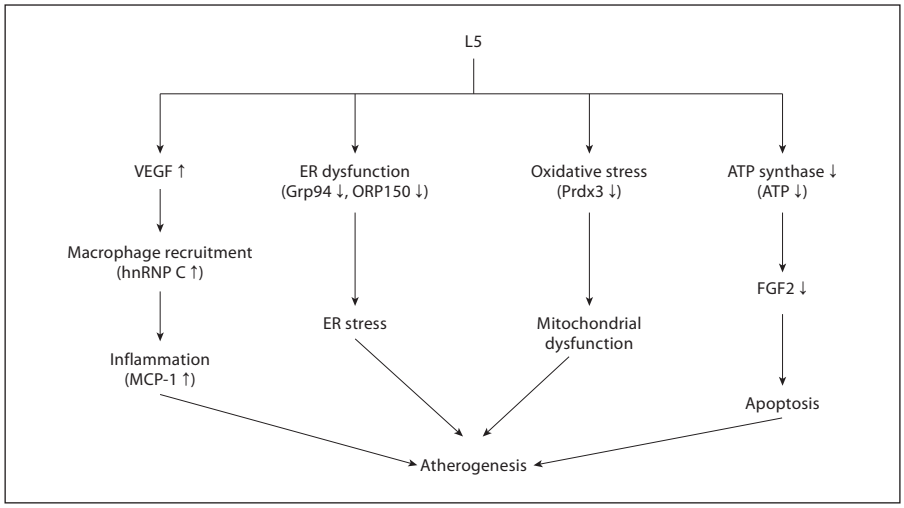

Fig. 6. A schematic illustrating how L5-induced cell stress may potentiate atherogenesis through the proteins identified in our study.

Our study highlights the effects of LDL charge in inducing cellular stress. Previously, it has been shown that the total protein concentration in L5 subfractions was 50% higher than that in L1 subfractions [37]. L5 showed distinctive biologic and physicochemical properties from L1. Furthermore, L5 contained greater concentrations of apoE, apoAI, apoCIII, and fragmented apoB100, which may contribute to the electronegativity of L5 [16, 37]. Further studies are necessary to determine the composition and unique modifications of L5 that contribute to its negative charge and, potentially, its cytotoxic effects. In addition, studies are warranted that aim to identify the active components of L5, such as phospholipids and derivatives (e.g. platelet-activating factor-like lipids and lysolecithins [15, 52]).

In summary, we showed that L5, but not L1, induced stress in HUVECs by causing inflammation and mitochondrial dysfunction (fig. 6). Furthermore, we confirmed the altered expression of proteins induced by L5 but not L1. Based on the known functions of these proteins, we pinpoint potential key players in the activation of cellular stress that leads to inflammation and apoptosis and may contribute to the initiation of atherogenesis.

Acknowledgments

The authors thank Nicole Stancel, PhD, of the Texas Heart Institute at St. Luke's Episcopal Hospital, for editorial assistance in the preparation of this paper.

This work was funded in part by research grants NSC-94-2314-B-002-001 (Lee), NSC-98-2314-B-002-121-MY3 (Hsu), and NSC-100-2314-B-039-040-MY3 (C.-H. Chen) from the National Science Council of Taiwan; a research grant from the Philip Morris External Research Program (C.-H. Chen); research grant 1-04-RA-13 from the American Diabetes Association (C.-H. Chen); research grant HL-63364 (Yang) from the National Institutes of Health, and research grant DOH101-TD-B-111-004 (C.-H. Chen) from the Taiwan Department of Health Clinical Trial and Research Center of Excellence. D. Tang is supported by training grant HL07812-10 from the National Institutes of Health.

References

1 Hermann J, Gulati R, Napoli C, Woodrum JE, Lerman LO, Rodriguez-Porcel M, Sica V, Simari RD, Ciechanover A, Lerman A: Oxidative stress-related increase in ubiquitination in early coronary atherogenesis. FASEB J 2003;17:1730–1732.

2 Nuszkowski A, Grabner R, Marsche G, Unbehaun A, Malle E, Heller R: Hypochlorite-modified low density lipoprotein inhibits nitric oxide synthesis in endothelial cells via an intracellular dislocalization of endothelial nitric-oxide synthase. J Biol Chem 2001;276:14212–14221.

3 Sata M, Walsh K: Endothelial cell apoptosis induced by oxidized LDL is associated with the down-regulation of the cellular caspase inhibitor FLIP. J Biol Chem 1998;273:33103–33106.

4 Sonoki K, Yoshinari M, Iwase M, Iino K, Ichikawa K, Ohdo S, Higuchi S, Iida M: Glycoxidized low-density lipoprotein enhances monocyte chemoattractant protein-1 mRNA expression in human umbilical vein endothelial cells: relation to lysophosphatidylcholine contents and inhibition by nitric oxide donor. Metabolism 2002;51:1135–1142.

5 Madamanchi NR, Runge MS: Mitochondrial dysfunction in atherosclerosis. Circ Res 2007;100:460–473.
6 Nonn L, Berggren M, Powis G: Increased expression of mitochondrial peroxiredoxin-3 (thioredoxin peroxidase-2) protects cancer cells against hypoxia and drug-induced hydrogen peroxide-dependent apoptosis. Mol Cancer Res 2003;1:682–689.
7 Wonsey DR, Zeller KI, Dang CV: The c-Myc target gene PRDX3 is required for mitochondrial homeostasis and neoplastic transformation. Proc Natl Acad Sci USA 2002;99:6649–6654.
8 Gaubatz JW, Gillard BK, Massey JB, Hoogeveen RC, Huang M, Lloyd EE, Raya JL, Yang CY, Pownall HJ: Dynamics of dense electronegative low density lipoproteins and their preferential association with lipoprotein phospholipase A_2. J Lipid Res 2007;48:348–357.
9 Chen HH, Chen CY, Chow LP, Chen CH, Lee YT, Smith CV, Yang CY: Iron-catalyzed oxidation of Trp residues in low-density lipoprotein. Biol Chem 2011;392:859–867.
10 Lu J, Yang JH, Burns AR, Chen HH, Tang D, Walterscheid JP, Suzuki S, Yang CY, Sawamura T, Chen CH: Mediation of electronegative low-density lipoprotein signaling by LOX-1: a possible mechanism of endothelial apoptosis. Circ Res 2009;104:619–627.
11 Devries-Seimon T, Li Y, Yao PM, Stone E, Wang Y, Davis RJ, Flavell R, Tabas I: Cholesterol-induced macrophage apoptosis requires ER stress pathways and engagement of the type A scavenger receptor. J Cell Biol 2005;171:61–73.
12 Li Y, Schwabe RF, DeVries-Seimon T, Yao PM, Gerbod-Giannone MC, Tall AR, Davis RJ, Flavell R, Brenner DA, Tabas I: Free cholesterol-loaded macrophages are an abundant source of tumor necrosis factor-α and interleukin-6: model of NF-κB- and MAP kinase-dependent inflammation in advanced atherosclerosis. J Biol Chem 2005;280:21763–21772.
13 Rao RV, Peel A, Logvinova A, del Rio G, Hermel E, Yokota T, Goldsmith PC, Ellerby LM, Ellerby HM, Bredesen DE: Coupling endoplasmic reticulum stress to the cell death program: role of the ER chaperone GRP78. FEBS Lett 2002;514:122–128.
14 Yang CY, Raya JL, Chen HH, Chen CH, Abe Y, Pownall HJ, Taylor AA, Smith CV: Isolation, characterization, and functional assessment of oxidatively modified subfractions of circulating low-density lipoproteins. Arterioscler Thromb Vasc Biol 2003;23:1083–1090.
15 Chen CH, Jiang T, Yang JH, Jiang W, Lu J, Marathe GK, Pownall HJ, Ballantyne CM, McIntyre TM, Henry PD, Yang CY: Low-density lipoprotein in hypercholesterolemic human plasma induces vascular endothelial cell apoptosis by inhibiting fibroblast growth factor 2 transcription. Circulation 2003;107:2102–2108.
16 Yang CY, Raya JL, Chen HH, Chen CH, Abe Y, Pownall HJ, Taylor AA, Smith CV: Isolation, characterization, and functional assessment of oxidatively modified subfractions of circulating low-density lipoproteins. Arterioscler Thromb Vasc Biol 2003;23:1083–1090.
17 Chen HH, Hosken BD, Huang M, Gaubatz JW, Myers CL, Macfarlane RD, Pownall HJ, Yang CY: Electronegative LDLs from familial hypercholesterolemic patients are physicochemically heterogeneous but uniformly proapoptotic. J Lipid Res 2007;48:177–184.
18 Lu J, Jiang W, Yang JH, Chang PY, Walterscheid JP, Chen HH, Marcelli M, Tang D, Lee YT, Liao WS, Yang CY, Chen CH: Electronegative LDL impairs vascular endothelial cell integrity in diabetes by disrupting fibroblast growth factor 2 (FGF2) autoregulation. Diabetes 2008;57:158–166.
19 Tang D, Lu J, Walterscheid JP, Chen HH, Engler DA, Sawamura T, Chang PY, Safi HJ, Yang CY, Chen CH: Electronegative LDL circulating in smokers impairs endothelial progenitor cell differentiation by inhibiting Akt phosphorylation via LOX-1. J Lipid Res 2008;49:33–47.
20 De Castellarnau C, Sanchez-Quesada JL, Benitez S, Rosa R, Caveda L, Vila L, Ordonez-Llanos J: Electronegative LDL from normolipemic subjects induces IL-8 and monocyte chemotactic protein secretion by human endothelial cells. Arterioscler Thromb Vasc Biol 2000;20:2281–2287.
21 Tai MH, Kuo SM, Liang HT, Chiou KR, Lam HC, Hsu CM, Pownall HJ, Chen HH, Huang MT, Yang CY: Modulation of angiogenic processes in cultured endothelial cells by low density lipoproteins subfractions from patients with familial hypercholesterolemia. Atherosclerosis 2006;186:448–457.
22 Chen CY, Lee CM, Hsu HC, Yang CY, Chow LP, Lee YT: Proteomic approach to study the effects of various oxidatively modified low-density lipoprotein on regulation of protein expression in human umbilical vein endothelial cell. Life Sci 2007;80:2469–2480.
23 Miyagi T, Hori O, Koshida K, Egawa M, Kato H, Kitagawa Y, Ozawa K, Ogawa S, Namiki M: Antitumor effect of reduction of 150-kDa oxygen-regulated protein expression on human prostate cancer cells. Int J Urol 2002;9:577–585.
24 Rose K, Gast RE, Seeger A, Krieglstein J, Klumpp S: ATP-dependent stabilization and protection of fibroblast growth factor 2. J Biotechnol 2010;145:54–59.
25 Rose K, Pallast S, Klumpp S, Krieglstein J: ATP-binding on fibroblast growth factor 2 partially overlaps with the heparin-binding domain. J Biochem 2008;144:343–347.
26 Moser TL, Kenan DJ, Ashley TA, Roy JA, Goodman MD, Misra UK, Cheek DJ, Pizzo SV: Endothelial cell surface F1-F0 ATP synthase is active in ATP synthesis and is inhibited by angiostatin. Proc Natl Acad Sci USA 2001;98:6656–6661.
27 Martinez LO, Jacquet S, Esteve JP, Rolland C, Cabezon E, Champagne E, Pineau T, Georgeaud V, Walker JE, Terce F, Collet X, Perret B, Barbaras R: Ectopic beta-chain of ATP synthase is an apolipoprotein A-I receptor in hepatic HDL endocytosis. Nature 2003;421:75–79.
28 Martinez LO, Jacquet S, Terce F, Collet X, Perret B, Barbaras R: New insight on the molecular mechanisms of high-density lipoprotein cellular interactions. Cell Mol Life Sci 2004;61:2343–2360.
29 Chang TS, Cho CS, Park S, Yu S, Kang SW, Rhee SG: Peroxiredoxin III, a mitochondrion-specific peroxidase, regulates apoptotic signaling by mitochondria. J Biol Chem 2004;279:41975–41984.
30 Zhang H, Luo Y, Zhang W, He Y, Dai S, Zhang R, Huang Y, Bernatchez P, Giordano FJ, Shadel G, Sessa WC, Min W: Endothelial-specific expression of mitochondrial thioredoxin improves endothelial cell function and reduces atherosclerotic lesions. Am J Pathol 2007;170:1108–1120.
31 Dreyfuss G, Kim VN, Kataoka N: Messenger-RNA-binding proteins and the messages they carry. Nat Rev Mol Cell Biol 2002;3:195–205.
32 Dreyfuss G, Matunis MJ, Pinol-Roma S, Burd CG: hnRNP proteins and the biogenesis of mRNA. Annu Rev Biochem 1993;62:289–321.
33 Garneau D, Revil T, Fisette JF, Chabot B: Heterogeneous nuclear ribonucleoprotein F/H proteins modulate the alternative splicing of the apoptotic mediator Bcl-x. J Biol Chem 2005;280:22641–22650.
34 Kim JH, Paek KY, Choi K, Kim TD, Hahm B, Kim KT, Jang SK: Heterogeneous nuclear ribonucleoprotein C modulates translation of c-myc mRNA in a cell cycle phase-dependent manner. Mol Cell Biol 2003;23:708–720.
35 Hossain MN, Fuji M, Miki K, Endoh M, Ayusawa D: Downregulation of hnRNP C1/C2 by siRNA sensitizes HeLa cells to various stresses. Mol Cell Biochem 2007;296:151–157.
36 Tang D, Lu J, Walterscheid JP, Chen HH, Engler DA, Sawamura T, Chang PY, Safi HJ, Yang CY, Chen CH: Electronegative LDL circulating in smokers impairs endothelial progenitor cell differentiation by inhibiting Akt phosphorylation via LOX-1. J Lipid Res 2008;49:33–47.
37 Yang CY, Chen HH, Huang MT, Raya JL, Yang JH, Chen CH, Gaubatz JW, Pownall HJ, Taylor AA, Ballantyne CM, Jenniskens FA, Smith CV: Pro-apoptotic low-density lipoprotein subfractions in type II diabetes. Atherosclerosis 2007;193:283–291.
38 Linnik KM, Herscovitz H: Multiple molecular chaperones interact with apolipoprotein B during its maturation. The network of endoplasmic reticulum-resident chaperones (ERp72, GRP94, calreticulin, and BiP) interacts with apolipoprotein B regardless of its lipidation state. J Biol Chem 1998;273:21368–21373.

39 Zhang J, Herscovitz H: Nascent lipidated apolipoprotein B is transported to the Golgi as an incompletely folded intermediate as probed by its association with network of endoplasmic reticulum molecular chaperones, GRP94, ERp72, BiP, calreticulin, and cyclophilin B. J Biol Chem 2003;278:7459–7468.
40 Qiu W, Kohen-Avramoglu R, Mhapsekar S, Tsai J, Austin RC, Adeli K: Glucosamine-induced endoplasmic reticulum stress promotes ApoB100 degradation: evidence for Grp78-mediated targeting to proteasomal degradation. Arterioscler Thromb Vasc Biol 2005;25:571–577.
41 Ozcan U, Cao Q, Yilmaz E, Lee AH, Iwakoshi NN, Ozdelen E, Tuncman G, Gorgun C, Glimcher LH, Hotamisligil GS: Endoplasmic reticulum stress links obesity, insulin action, and type 2 diabetes. Science 2004;306:457–461.
42 Ye R, Jung DY, Jun JY, Li J, Luo S, Ko HJ, Kim JK, Lee AS: Grp78 heterozygosity promotes adaptive unfolded protein response and attenuates diet-induced obesity and insulin resistance. Diabetes 2010;59:6–16.
43 Pozza LM, Austin RC: Getting a GRP on tissue factor activation. Arterioscler Thromb Vasc Biol 2005;25:1529–1531.
44 Feaver RE, Hastings NE, Pryor A, Blackman BR: GRP78 upregulation by atheroprone shear stress via p38-, $\alpha_2\beta_1$-dependent mechanism in endothelial cells. Arterioscler Thromb Vasc Biol 2008;28:1534–1541.
45 Wu HL, Li YH, Lin YH, Wang R, Li YB, Tie L, Song QL, Guo DA, Yu HM, Li XJ: Salvianolic acid B protects human endothelial cells from oxidative stress damage: a possible protective role of glucose-regulated protein 78 induction. Cardiovasc Res 2009;81:148–158.
46 Jorgensen MM, Jensen ON, Holst HU, Hansen JJ, Corydon TJ, Bross P, Bolund L, Gregersen N: Grp78 is involved in retention of mutant low density lipoprotein receptor protein in the endoplasmic reticulum. J Biol Chem 2000;275:33861–33868.
47 Berwin B, Delneste Y, Lovingood RV, Post SR, Pizzo SV: SREC-I, a type F scavenger receptor, is an endocytic receptor for calreticulin. J Biol Chem 2004;279:51250–51257.
48 Sanson M, Auge N, Vindis C, Muller C, Bando Y, Thiers JC, Marachet MA, Zarkovic K, Sawa Y, Salvayre R, Negre-Salvayre A: Oxidized low-density lipoproteins trigger endoplasmic reticulum stress in vascular cells: prevention by oxygen-regulated protein 150 expression. Circ Res 2009;104:328–336.
49 Arrington DD, Schnellmann RG: Targeting of the molecular chaperone oxygen-regulated protein 150 (ORP150) to mitochondria and its induction by cellular stress. Am J Physiol Cell Physiol 2008;294:C641–C650.
50 Ron D: Translational control in the endoplasmic reticulum stress response. J Clin Invest 2002;110:1383–1388.
51 Chang PY, Lu SC, Lee CM, Chen YJ, Dugan TA, Huang WH, Chang SF, Liao WS, Chen CH, Lee YT: Homocysteine inhibits arterial endothelial cell growth through transcriptional downregulation of fibroblast growth factor-2 involving G protein and DNA methylation. Circ Res 2008;102:933–941.
52 Kugiyama K, Kerns SA, Morrisett JD, Roberts R, Henry PD: Impairment of endothelium-dependent arterial relaxation by lysolecithin in modified low-density lipoproteins. Nature 1990;344:160–162.